ME525 Applied Acoustics Lecture 26, Winter 2024
Range dependence and adiabatic modes

Peter H. Dahl, University of Washington

A Range-dependent waveguide and mode cut-off

Problems studied thus far using normal modes are based on range-independent waveguide, where, although sound speed can change with depth (e.g., see Fig. 3 of Lecture 24), neither depth nor sound speed conditions change with range. This is a reasonable approximation for many problems but there are many instances where the approximation fails. One is the problem of upslope propagation where a sound source is off shore and the bathymetry is gradually changing towards shore. Jensen and Kuperman (1980) first addressed this problem for the idealized case of sound propagation in waters of depth 200 m over the first 5 km of range, after which the depth reduces linearly to effectively 0 m at range 12 km from the original source (Fig. 1). To solve this problem they used, instead of normal modes, the parabolic wave equation (PE) approach which is directly amenable to solving range dependent problems. For more details on the PE approach the text by Jensen, Kuperman, Porter and Schmidt (2011) is an excellent starting point.

However for given range independent waveguide the complex acoustic field, or $g(r, z, z_s)$ produced by the PE is similar (within a very close approximation) to that produced by normal modes, even though normal modes are not an output of PE computations *per se*. For example, in Fig. 1 observe an interference pattern with depth in effect over the first 5 km that is suggestive of 3 trapped modes. Once the depth begins to change (reduce) modes begin to "cut off" one by one, starting with the first mode.

Seeing the modes cut-off in order of mode number $n = 3, 2, 1$ it's interesting to check out the formula for the approximate number of trapped modes in a underwater waveguide given in Eq.(2) of Lecture 25. Using the parameters of the problem, including frequency 25 Hz, Fig. 2 seems reasonably predictive concerning the water depth interval that can support 3 modes, then 2 modes, then 1 mode, and ultimately 0 modes.

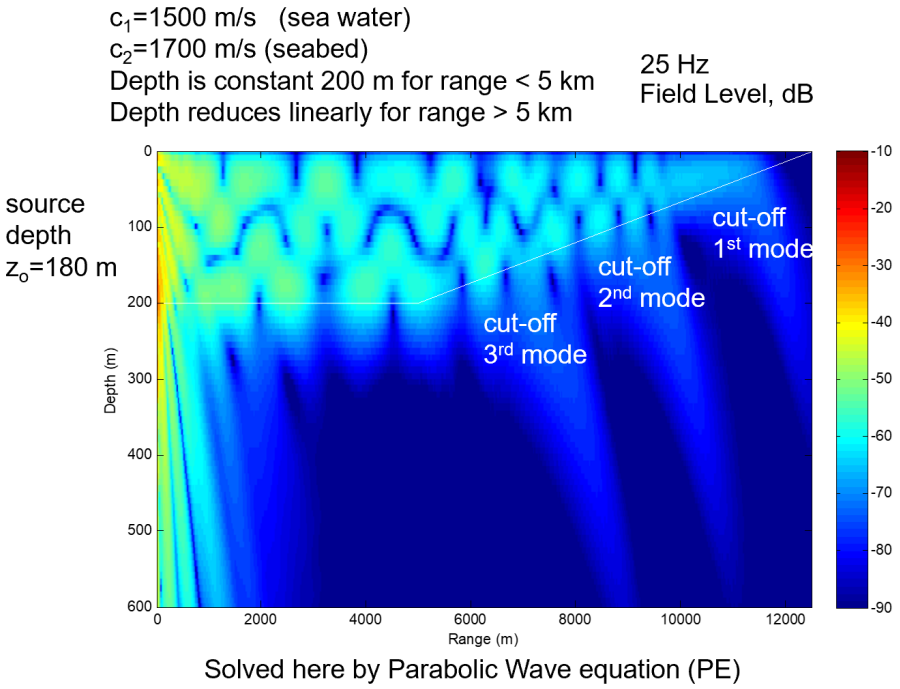

Figure 1: Modes in waveguide of depth 200 m up to range 5 km, after which there is a gradual decrease in depth following Jensen Kuperman problem (1980). Thin, white line shows the changing depth with range. Three trapped modes are originally supported for 25 Hz source within the 200 m depth region. As depth decreases modes begin to cut-off starting with highest mode first. Eventually no modes can propagate in this waveguide. Simulation by P. H. Dahl using parabolic wave equation.

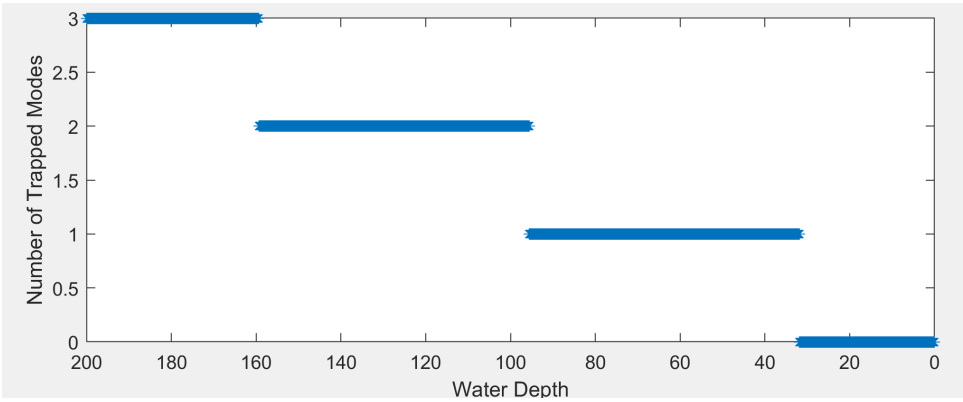

Figure 2: Number of trapped modes estimated by Eq. (2) of Lecture 25, for the waveguide shown in Fig. 1 based on water depth H reducing from 200 m to 0 m.

Adiabatic modes

One way to handle a degree of range-dependence using normal modes is through the technique know as *adiabatic modes*. Indeed the problem in Fig. 1 can be solved in this manner. The basic idea is that the acoustic field is determined by (i) conditions (e.g., water depth, sound speed and density properties) in effect at source range, (ii) conditions at the receiver range, and (ii) and some average

of the conditions between these two points. For (iii) this average for a given mode n is characterized by the *average* horizontal wavenumber $\overline{k_{rn}}$ between these two points. It is not hard to implement, and good starting reference is Kuperman and Roux (2007).

To a simple example is the geometry of the Nantucket experiment (Fig. 3). A source is placed at depth 6.1 m in waters 14.6 m deep. This depth is maintained for about 660 m, after which the depth reduces to 13.9 m. A receiver is another 660 m downrange at depth 12.5 m. So, approximately the first half the waveguide has $H = 14.9$ m and second half has $H = 13.9$ m. Thus the average horizontal wavenumber $\overline{k_{rn}}$ will be given by $0.5(k^1_{rn} + k^2_{rn}$ where $1, 2$ identify the first and second half of the propagation range, respectively. In this case $1, 2$ also correspond to the conditions as the source and receiver, respectively. This is a particularly simple case where the average of just two horizontal wavenumber is needed. In general there may some waited average, e.g. were the propagation range not divided evenly into two parts. Using this technique to solve the wedge problem in Fig. 1 requires many "stair steps" to approximate the slope and the appropriate average must be taken.

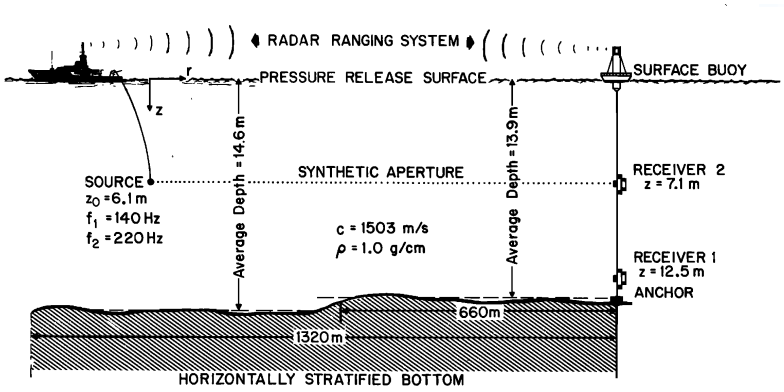

Figure 3: Geometry of experiment off Nantucket. Figure is Fig. 1 of Frisk, Lynch and Rajan (1989).

The adiabatic solution which accommodates (i-iii) is given by modifying Eq.(5) of Lecture 25 to

$$g(r, z, z_s) = \frac{\pi i}{\rho_1} \sum_n A^r_n \sin(\gamma^r_n z) A^s_n \sin(\gamma^s_n z_s) H^1_0(\overline{k_{rn}} r). \tag{1}$$

The key differences are: rather than A^2_n, there are A^s_n and A^r_n computed separately based on conditions at the source s and receiver r, similarly, instead of γ_n there is γ^s_n and γ^r_n, and finally there is $\overline{k_{rn}}$.

Taking the Nantucket geometry, with frequency 220 Hz $c_w = 1503$ m/s and $c_b = 1700$ m/s, $\rho_w, rho_b = 1000$ and 1500 kg/m^3 respectively, I produced a simple adiabatic result (Fig. 4) for source depth 6.1 m and receiver depth 12.5 m. The effect of the change in depth for this two-mode pattern is transition in modal interference at range 660 m which occurs smoothly.

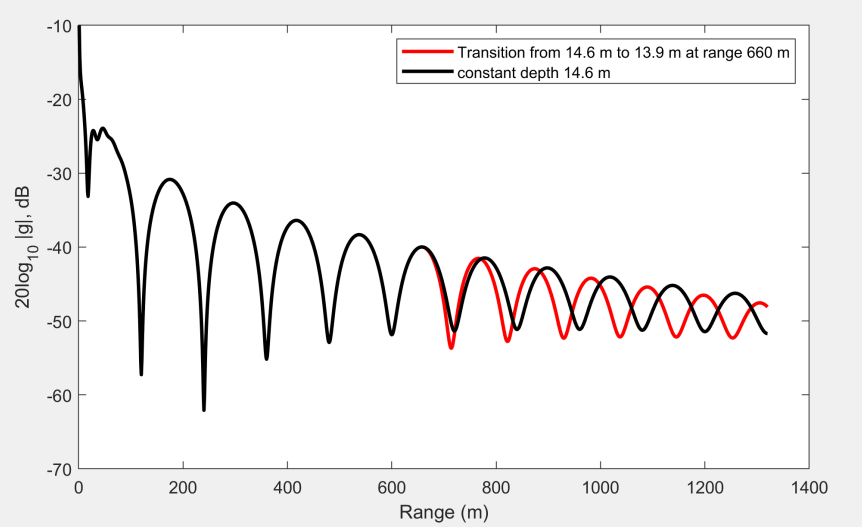

Figure 4: Geometry of experiment off Nantucket. Figure is Fig. 1 of Frisk, Lynch and Rajan (1989).

References

F.B. Jensen, W.A. Kuperman, Sound propagation in a wedge-shaped ocean with a penetrable bottom. J. Acoust. Soc. Am. 67, 1564–1566 (1980)

F. Jensen, W. Kuperman, M. Porter, and H. Schmidt, *Computational Ocean Acoustics*, (Springer, New York, 2011)

W.A. Kuperman and P. Roux, Propagation of Sound, In: Springer Handbook of Acoustics, T. D. Rossing (Ed.), (Springer, 2007)

Frisk, G. V., J. Lynch and S. Rajan, "Determination of the compressional wave speed profiles using modal inverse techniques in a range-dependent environment in Nantucket sound," *J. Acoust. Soc. Am.* 86, Nov. 1989.

ME525 Applied Acoustics Lecture 27, Winter 2024
Mode group and phase velocity

Peter H. Dahl, University of Washington

Mode group and phase velocity

An important property of underwater acoustic waveguide propagation is the phenomenon of the speed of energy transport for a given mode, which depends on frequency. Since the modes depend on geometry, i.e., primarily water depth H, this is known as geometric dispersion (e.g. Frisk, 1994).

An initial pathway towards understanding this is to revert to the original, simplified problem of a waveguide with rigid boundary conditions. Revisit Table 1 of Lecture 24, find the horizontal wavenumbers k_{rn} for modes 1 and 2 to be 1.0280 and 0.9271, respectively. Corresponding "preferred angles" for these two modes as defined by $k_{rn}\cos\theta_n = k$ are 8.7°, 29.9°, respectively based on the frequency, 240 Hz, and water sound speed, 1450 m/s, which establish k. Imagine next mode 1 traveling down the waveguide via its equivalent "ray", with horizontal angle 8.7°, reflecting off the rigid seabed boundary and air-water boundary at this same angle. This applies to mode 2 but now the angle is 29.9°. Evidently the speed by which mode 1 propagates through the waveguide is faster than mode 2 given mode 1 has fewer up/down cycles since the equivalent ray is more horizontal. Thus, mode 1 has a faster group velocity than mode 2 for this particular example.

The above is simplified but gets the point across although the topic of group velocity is considerably more complicated. Additional insight is found by studying the propagation of a short pulse of sound consisting of many frequencies all initially transmitted at once. An example of this so-called broadband pulse is sound from an explosive source. Figure 1 (upper) shows a simulated time series for such a broadband pulse, at range 12000 m based on conditions approximated by a Pekeris waveguide with water speed $c_w = 1468$m/s, sediment speed $c_b = 1830$ m/s and water depth $H = 74$ m.

Observe that the "main" pulse arrives after a delay of abou 8 s, consistent with nominal value of range divided by c_w. However prior to the main pulse there exists low-amplitude arrival which slowly grows in amplitude. This is the ground wave which has traveled at the faster speed in the sea bed. The pulse continues to evolve, with different frequency content arriving at different times. This is dispersion.

This evolution of time and frequency properties for the arrival of the pulse is seen with time-frequency analysis based on a spectrogram of the simulated time series (Fig. 1, lower). This shows the evolving mode structure: mode 1 is spans the largest frequency range (left side of spectrogram) and mode 5 the smallest frequency range (upper right of spectrogram). To further clarify, use

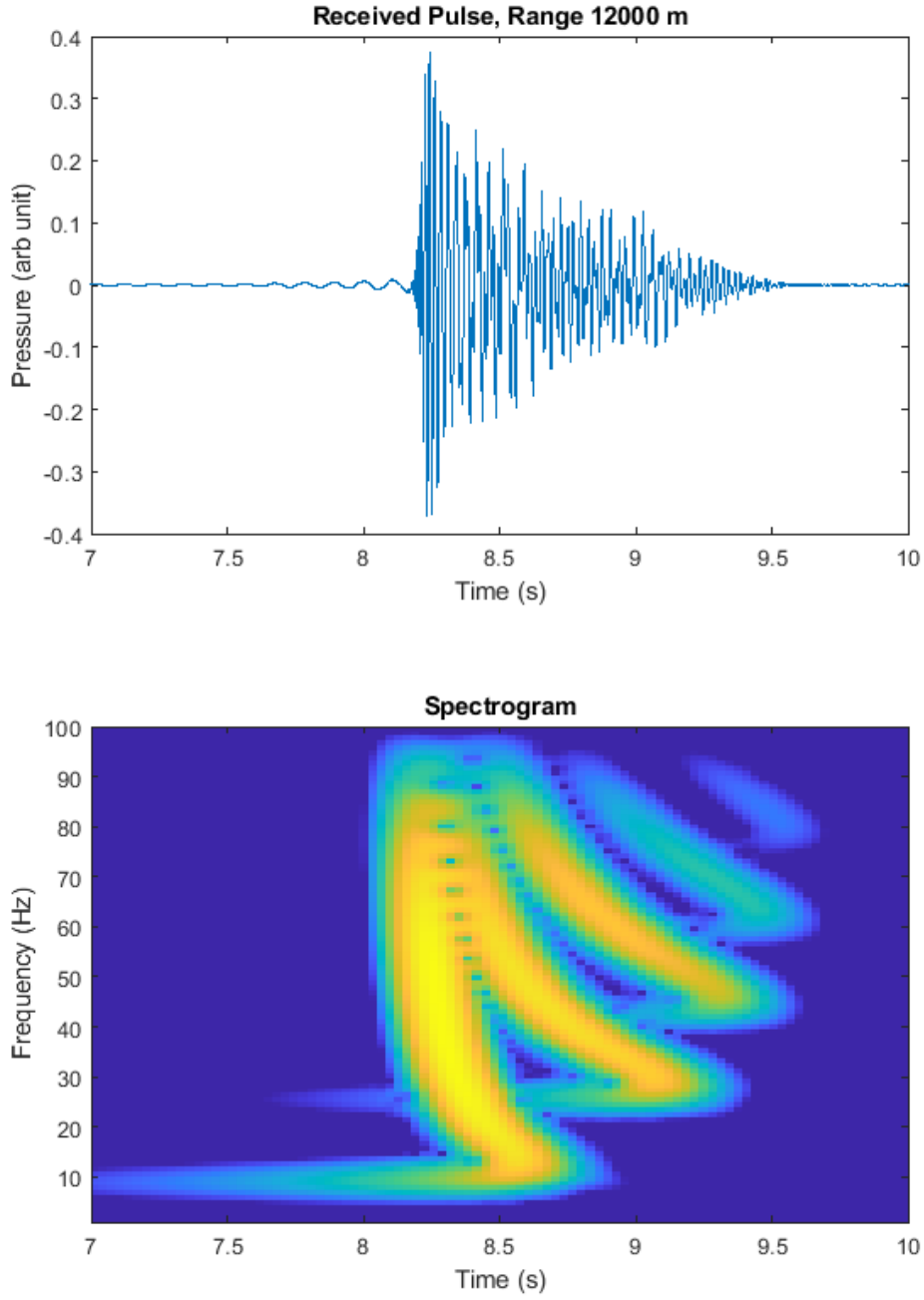

Figure 1: Upper: synthetic broad band pulse computed for received range of 12000 m for the Pekeris waveguide discussed in text. Lower: spectrogram of the received pulse showing 5 modes.

again the formula for approximate number of trapped modes Eq. (2) of Lecture 25. This equation produces the five frequencies: 9, 25, 41, 58 and 74 Hz representing the approximate onset of modes 1 through 5, respectively. For example, below about 9 Hz, there appears to be little on no energy

support in the spectrogram, and thus ~ 9 Hz is the cut-off frequency for mode 1 for this waveguide. Similarly the support is missing below about 25 Hz for mode 2, and so on.

Furthermore mode 1 arrives first: starting about 7 sec at low amplitude, reaching higher amplitude at about 8 sec. Mode 5 arrives last with its influence not seen until after 9 sec. Thus we can intuit that mode 1 generally has faster *group velocity*, $V_n, n = 1$ than mode 5, not unlike the previous simple example based on increasing propagation angles for increasing mode number.

Imagine now turning the pattern in Fig. 1 (lower) 90° clockwise, so time is on the vertical axis, and 8 s represents a faster speed than 8.5 s and so on. For example 8 s corresponds to approximately 1400 m/s and 9 s to approximately 1300 m/s. This rotated figure represents the dispersion curves as function of frequency f for modes 1-5, or $V_n(f)$ n =1 to 5. The exact set of dispersion curves for this case through modes 1-4 are shown in Fig. 2. Note this figure also includes the phase velocities C_n–these are simple to compute: given the horizontal wavenumber for each mode k_{rn}, then $C_n = \frac{\omega}{k_{rn}}$. The very interesting minimum in $V_n(f)$ for each mode is known as the Airy phase.

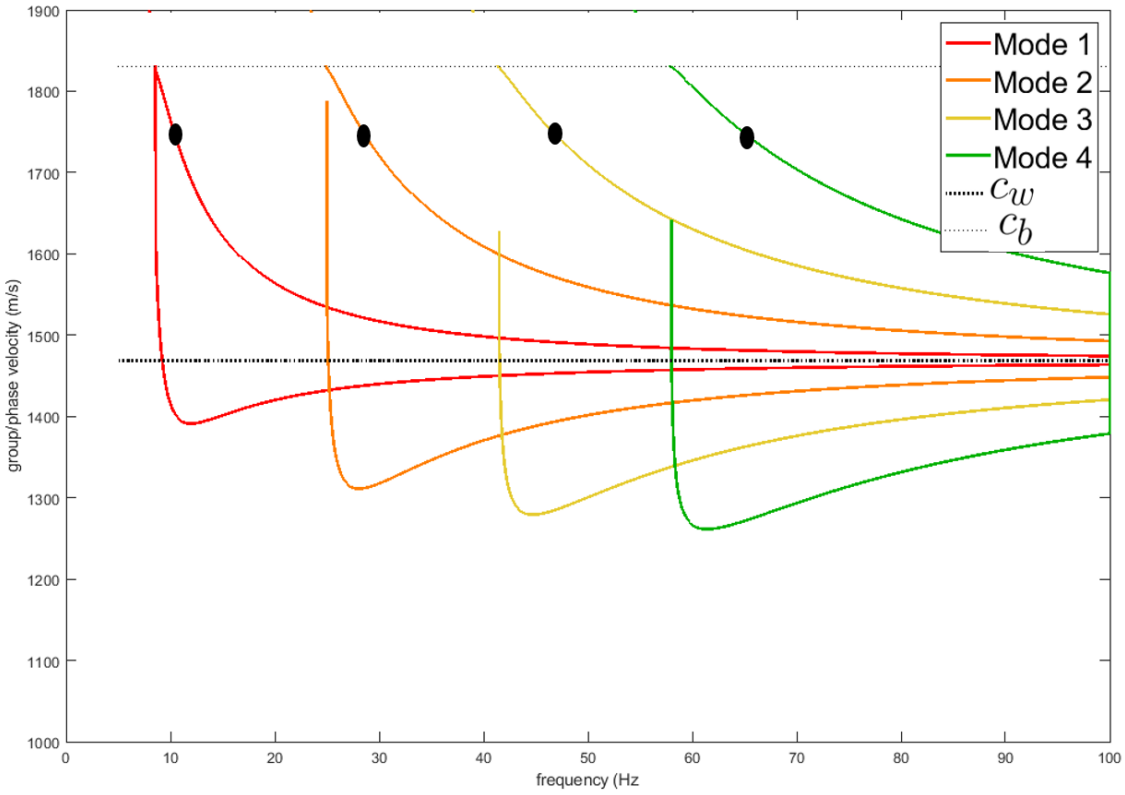

Figure 2: Theoretical curves for group $V_n(f)$ and phase $C_n(f)$ velocity as a function of frequency for modes 1-4, for the waveguide properties discussed in text. Phase velocity curves are distinguished by the black symbol place on each curve. Lower horizontal dashed line equals water speed c_w and upper horizontal dashed line equals the seabed speed c_b; all group velocity curves theoretically reach the higher seabed speed though some curves do not owing to numerical issues.

It can be observed in real data representing the reception of an initially broad pulse, such as from an explosive source or air gun used in geophysical exploration, after that pulse has traveled a sufficient range for dispersion to be observed. Examine now closely the time-series simulation in Fig. 1 around time 8.5 s and 9 s, where the frequency appears to be somewhat lower. These regions likely correspond to the Airy phase contribution from modes 1 and 2, respectively.

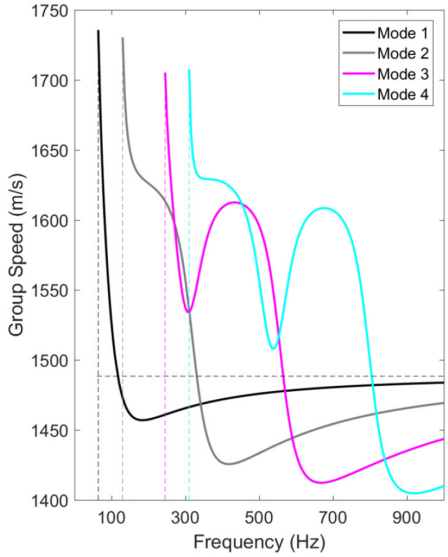

Figure 3: Theoretical curves for group $V_n(f)$ and phase $C_n(f)$ velocity as a function of frequency for modes 1-4, for the waveguide properties discussed in text. Phase velocity curves are distinguished by the black symbol. All group velocity curves theoretically reach the higher seabed speed c_2 though some curves do not owing to numerical issues.

Figure 2 is a somewhat classic figure showing group $V_n(f)$ and phase $C_n(f)$ velocities for a Pekeris waveguide where the sound speed in the seabed is constant. For these conditions each mode supported has one Airy phase region representing the minimum group velocity for that mode. The group velocity in this Airy phase region is relatively constant of over band of frequencies or *stationary*. The view in Fig. 2 is both a useful and parsimonious model with which to compare with observations, particularly if there is little known about the seabed properties. However, more complex seabed sound variation, such a sediment layer within sediment sound varies with a linear gradient, can produce group velocity curves $V_n(f)$ that manifest multiple stationary regions, corresponding to both high and low group velocities. An example (Fig. 3) is for conditions represented by $c_w = 1488.5$ m/s and $c_b = 1630 + az$ over the first 20 m of sediment where the gradient $a = 6^1$ s and z is sediment depth; for sediment depth greater than 20 m $c_b = 1740$ m/s. In this case modes 3 and 4 show two Airy phase regions.

One standard way to compute V_n is through the following formal definition:

$$V_n = \frac{d\omega}{dk_{rn}} \tag{1}$$

where k_{rn} is the horizontal wavenumber for the n^{th} mode. This can be quite delicate to compute numerically–typically one needs to evaluate modes over a fine frequency spacing, take the finite difference and hope it works. For the Pekeris waveguide involving just two media water and sediment, each with separate sound speeds and densities, Frisk (1994, pp. 152-154) also provides a handy analytical formulas, with results for the case under discussion shown in Fig. 2.

An interesting alternative way (Chapman and Ellis, 1983) is

$$V_n = \frac{\int_0^\infty U_n^2(z)/\rho(z)dz}{C_n \int_0^\infty U_n^2(z)/(\rho(z)c(z)^2)dz} \tag{2}$$

where $U_n(z)$ is the unique normal mode function at a given frequency. Check the dimension of Eq.(2)–does it make sense? Some care is still needed to evaluate this integral. For example, the behavior of the normal mode function for a more realistic Pekeris waveguide changes from $\sin(\gamma_n z)$ to decaying exponential for $z > H$ (see Fig. 4 of Lecture 25).

As a simple test, use the case of the rigid boundary condition on the seabed. Here, the integral in Eq.(2) is limited to between 0 and water depth H. The result (Fig. 4) for case of $H = 20$ m, and water sound speed of 1525 m/s for the first four modes shows that the cut-off frequency for this waveguide is about 19 Hz. Notice that V_n for this rigid boundary case are quite different from the Pekeris case in Fig. 2, with the notable absence of an Airy phase.

The phase velocities, however, are somewhat more realistic. Indeed this property is often exploited in a technique known as "warping" (Fig. 5), which takes a spectrogram from a received broadband signal and "warping" it, or straightening it, to follow the phase velocities of an "equivalent" rigid boundary waveguide. For example, the thin red lines in the lower right panel of Fig. 5 shows such phase velocities.

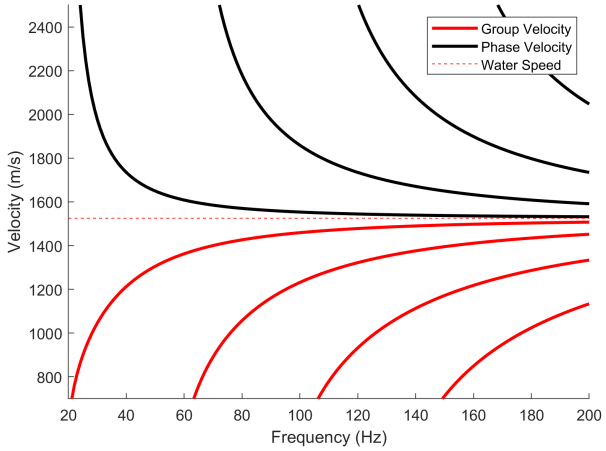

Figure 4: The group $V_n(f)$ and phase $C_n(f)$ velocities as a function of frequencies for waveguide of depth H 20 m, water speed 1525 m/s, and rigid boundary condition for water-seabed interface.

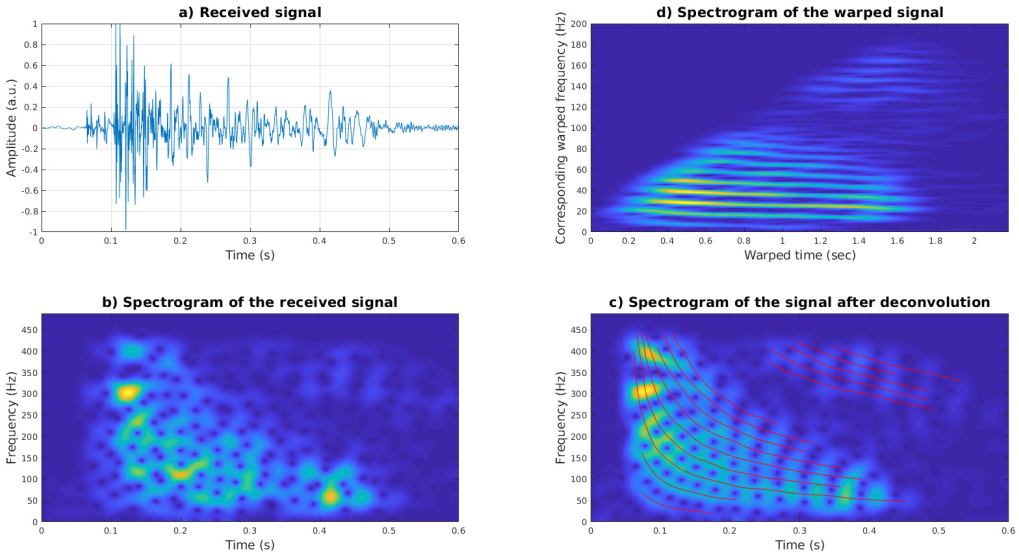

Figure 5: Figure supplied by my colleague Julien Bonnel, of Woods Hole Oceanographic Institution. See also Bonnel and Chapman, 2011.

References

Frisk, G. V. *Ocean and Seabed Acoustics* (Prentice Hall, Englewood Cliffs, NJ, 1994)

D. M. F. Chapman, and D.D. Ellis, "The group velocity of normal modes," *J. Acoust. Soc. Am.* 78, 983-979, 1983

J. Bonnel and N. R. Chapman, "Geoacoustic inversion in a dispersive waveguide using warping operators" *J. Acoust. Soc. Am.* EL101, 2011